J. Mech. Phys. Solids Vol. 33, No. 2, pp. 169–191, 1985.
Printed in Great Britain.

0022–5096/85 $3.00 + 0.00

HIGH STRAIN-RATE CRACK GROWTH IN RATE-DEPENDENT PLASTIC SOLIDS

L. B. FREUND

Division of Engineering, Brown University, Providence, RI 02912, U.S.A.

and

J. W. HUTCHINSON

Division of Applied Sciences, Harvard University, Cambridge, MA 02138, U.S.A.

(*Received* 12 *June* 1984)

ABSTRACT

AT HIGH crack velocities in metallic materials nearly all plastic strain accumulates at very high strain-rates, typically in the range $10^3\,s^{-1}$ to $10^5\,s^{-1}$. At these rates, dislocation motion is limited by dynamic lattice effects and the plastic strain-rate increases approximately linearly with stress. The problem for a crack growing at high velocity is posed for steady-state, small scale yielding in elastic/rate-dependent plastic solids. A general expression is derived for the near-tip stress intensity factor in terms of the remote intensity factor, or equivalently for the near-tip energy release-rate in terms of the overall release-rate. An approximate calculation of the plastic strain-rates provides this relation in analytical form. Imposition of the condition that the near-tip energy release-rate be maintained at a critical value provides a propagation equation for the growing crack. A single, nondimensional combination of material constants emerges as the controlling parameter. Implications for dynamic crack propagation are discussed.

1. INTRODUCTION

THE RESISTANCE of metals to plastic flow increases dramatically at very high strain-rates. The essence of cleavage in such materials is the ability of a crack to outrun almost all plastic deformation by virtue of the high strain-rates occurring near the rapidly advancing crack tip. Conditions for a crack to run at high velocity depend on the constitutive properties of the material, on the starting velocity of the nucleated crack, and on the overall crack driving force. The study of this paper is directed towards gaining understanding of these conditions by accounting for the rate-dependence of plastic flow in the analysis of high velocity crack growth. The results of the study are most obviously applicable to the propagation of cleavage cracks, but the theory also has implications for high velocity crack growth under other modes of fracture such as void growth and coalescence.

Rough estimates of the plastic strain-rates to be expected near the tip of a running crack are easily obtained. For crack velocities v which are less than about 40 or 50% of the elastic Rayleigh wave speed, the maximum extent of the active plastic zone can be estimated using quasi-static results. For small scale yielding crack growth in plane

strain under mode I conditions, the maximum extent of the plastic zone from the crack tip is approximately

$$R = 0.06(K/\tau_y)^2 \cong 0.14\mu G/\tau_y^2, \tag{1.1}$$

where K is the stress intensity factor, G is the elastic energy release-rate, μ is the elastic shear modulus and τ_y is the quasi-static yield stress in shear. For a crack running at velocity v, the maximum time any material element is subject to a stress above the yield stress is therefore no larger than R/v.

In quasi-static crack growth plastic strains develop near the tip which are many times the elastic strain at yield, $\gamma_y = \tau_y/\mu$. If a material element, which is engulfed by the outer portion of the active plastic zone of the running crack, experiences a plastic strain on the order of γ_y, then its average plastic strain-rate $\dot{\gamma}^p$ is on the order of

$$\dot{\gamma}^p \cong \gamma_y/(R/v) \cong 7v\tau_y^3/(\mu^2 G). \tag{1.2}$$

For a cleavage micro-crack in an iron single crystal, G is usually taken to be about 14 J/m^2. Using typical values of τ_y and taking v as one tenth of the Rayleigh wave speed, one finds that the estimate of $\dot{\gamma}^p$ from (1.2) is between 10^6/s and 10^7/s. Dynamic growth of a macroscopic cleavage crack in polycrystalline metals, such as steels at low temperatures, requires G-values which are more than 100 times greater than 14 J/m^2. Nevertheless, (1.2) still indicates very high plastic strain-rates in the range 10^4/s to 10^5/s for a rapidly running crack, and estimates based on material elements passing nearer to the tip will be even higher. Comparable values are also found for dynamic growth of a macro-crack in some of the less ductile metals which fail by hole growth and coalescence. The above estimates do not account for rate effects but they serve to set the stage for the present study.

Aspects of high strain-rate plasticity relevant to the present problem are discussed in Section 2, and some useful results from the elastic theory of dynamic crack growth are summarized in Section 3. The basic problem addressed in this paper is posed in Section 4, namely the high velocity steady-state growth of a crack in an elastic/rate-dependent plastic solid under conditions of small scale yielding. The constitutive relation of the solid is such that the near-tip stress field has an inverse square root singularity. A path independent line integral is introduced in Section 4 which facilitates the derivation of a general energy balance relating the near-tip energy release-rate, the overall energy release-rate, and the plastic dissipation. Estimates of the plastic strain-rates enable one to obtain the energy balance equation in analytical form, and this is carried out in Section 5 for the case of a plane strain crack in mode I. A propagation equation for the crack is obtained once the near-tip energy release-rate is specified. In this paper, propagation conditions are discussed for the case in which the near-tip energy release rate is maintained at a velocity-independent critical value. In Section 6 it is shown that the approximate calculation is actually exact in a certain asymptotic sense, and it is argued that the qualitative features which are revealed by the approximate analysis are likely to emerge from more accurate analyses as well. Nevertheless, the need for more complete analyses is also emphasized in Section 6. Speculation as to the relevance of the theory to the propagation of macro-cracks is illustrated in Section 7 with consideration of the temperature dependence of cleavage cracking of mild steel.

2. High Strain-rate Plasticity

Constitutive equations governing plastic flow in the several regimes of high strain-rate deformation have been compiled by Frost and Ashby (1982) for a wide variety of metals. The relations are visco-plastic in character with plastic strain-rate being a function of stress and temperature.

At an absolute temperature T below about one quarter of the melting temperature, the plot of shear stress, τ, vs plastic shear strain-rate, $\dot{\gamma}^p$, has the features shown in Fig. 1. At sufficiently high strain-rates ($\dot{\gamma}^p \geqslant \dot{\gamma}_t$, where $\dot{\gamma}_t$ is typically between 10^3/s and 10^4/s) dislocation motion is limited by dynamical responses inherent to the lattice known as phonon drag. In this regime an increase in plastic strain-rate is linearly proportional to an increase in stress, so that

$$\dot{\gamma}^p = \dot{\gamma}_t + \dot{\gamma}_0(\tau - \tau_t)/\mu \quad \text{for} \quad \tau \geqslant \tau_t, \tag{2.1}$$

where μ is the elastic shear modulus at the temperature in question and τ_t is the transition stress associated with $\dot{\gamma}_t$. The above form (2.1) is suggested by the data of Campbell and Ferguson (1970) for mild steel. The material constants $\dot{\gamma}_t$ and $\dot{\gamma}_0$ are relatively independent of temperature and the Campbell and Ferguson data give $\dot{\gamma}_t = 5 \times 10^3\ s^{-1}$ and $\dot{\gamma}_0 = 3 \times 10^7\ s^{-1}$.

At stresses below the transition stress dislocation motion is controlled by either lattice resistance or discrete obstacles. In either case, the stress dependence of the plastic strain-rate is much stronger than in the regime controlled by phonon drag. The plastic strain-rate drops by many orders of magnitude with a relatively small stress drop, as depicted in Fig. 1.

Temperature dependence can be quite strong in this intermediate strain-rate range, particularly for body centered cubic metals. For a pure α-iron, lattice resistance is the

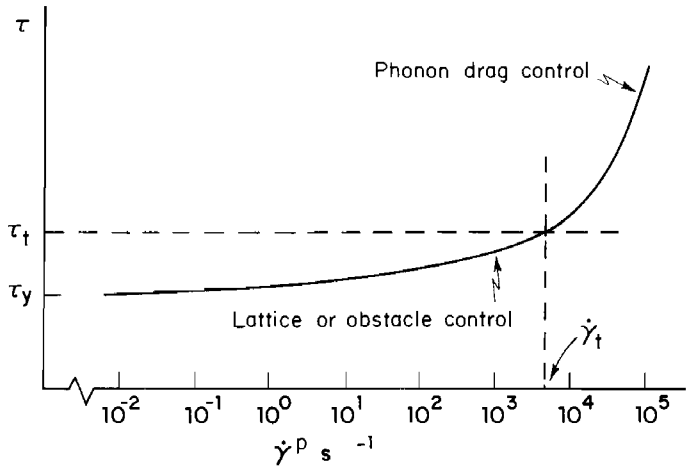

Fig. 1. Relation of stress to plastic strain-rate at a given temperature showing the transition between high strain-rate regime and low to intermediate strain-rate regime.

governing mechanism in this regime. Frost and Ashby give

$$\dot{\gamma}^p = c_p\left(\frac{\tau}{\mu}\right)^2 \exp-\left\{\frac{\Delta F_p}{kT}\left[1-\left(\frac{\tau}{\hat{\tau}}\right)^{3/4}\right]^{4/3}\right\} \quad \text{for} \quad \tau \leqslant \tau_t, \tag{2.2}$$

where $\hat{\tau}$ is the flow stress at 0 K. This parameter, the other parameters in (2.2), and the temperature dependence of μ are all presented in Table 8.1 in the book of Frost and Ashby. Using their values for α-iron, we have plotted curves of τ/μ vs plastic strain-rate in Fig. 2 for four temperatures. The transition stress τ_t was determined such that (2.2) coincides with $\dot{\gamma}_t$ at $\tau = \tau_t$, where Campbell and Ferguson's values for $\dot{\gamma}_t$ and $\dot{\gamma}_0$ were used. While $\dot{\gamma}_t$ has been taken to be independent of temperature, τ_t is seen to have a fairly strong temperature dependence.

Relations (2.1) and (2.2) will be used under transient conditions where a material element experiences a sudden stress elevation for a short period of time. The two relations were established for nominally steady-state deformation conditions and are associated with some characteristic strain level. More complicated constitutive relations strictly applicable to transient stressing are not available, at least not for quantitative application to problems such as the present one. The relatively simple relations (2.1) and (2.2) do capture the essence of high strain-rate plasticity and should be suitable for the purposes of the present study. In a recent survey, CLIFTON (1983) speculates on deviations from the simple descriptions used here.

To generalize the constitutive relation to multiaxial stress states, σ_{ij}, let

$$\tau = (\tfrac{1}{2}s_{ij}s_{ij})^{1/2}, \tag{2.3}$$

where s_{ij} is the stress deviator. Denote the pure shear visco-plastic relation charac-

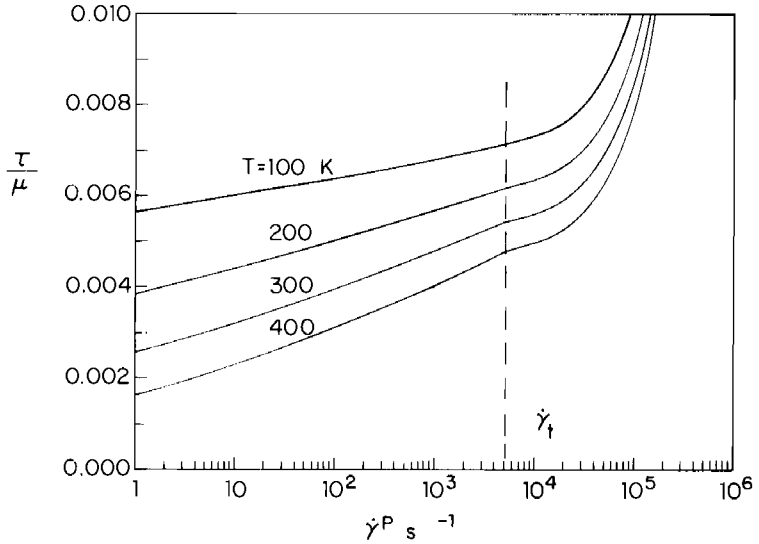

FIG. 2. Curves of stress as a function of plastic strain-rate at several temperatures for α-iron. See text for origin of data.

terized by (2.1) and (2.2) collectively by

$$\dot{\gamma}^p = F(\tau). \tag{2.4}$$

Then the plastic strain-rate under multiaxial stress states is taken to be

$$\dot{\varepsilon}_{ij}^p = \tfrac{1}{2}F(\tau)s_{ij}/\tau, \tag{2.5}$$

which reduces to (2.4) in pure shear. When τ drops below τ_y, the plastic strain-rate will be taken to be zero. This cutoff is somewhat arbitrary and will be seen to be immaterial in the analysis which follows.

The material is assumed to be elastically isotropic so that the elastic strain-rates are given by

$$\dot{\varepsilon}_{ij}^e = \frac{1+\nu}{E}\dot{\sigma}_{ij} - \frac{\nu}{E}\dot{\sigma}_{kk}\delta_{ij}, \tag{2.6}$$

where E is Young's modulus and ν is Poisson's ratio. The total strain-rate is the sum of the elastic and plastic parts.

3. Preliminaries from the Theory of Elastic Crack Propagation

A crack advances in its plane with velocity v in the x_1-direction under conditions of plane strain in mode I in an isotropic, linearly elastic solid. The singular stress field at the tip of the crack is given by

$$\sigma_{ij} = \frac{K}{\sqrt{(2\pi r)}}\Sigma_{ij}(\theta, m), \tag{3.1}$$

where K is the dynamic stress intensity factor and r and θ are planar-polar coordinates centered at the tip with θ measured from the x_1-axis. The functions Σ_{ij} are also functions of Poisson's ratio, ν, but ν will not be listed explicitly among the arguments, neither for Σ_{ij} nor for related functions introduced below. The crack Mach number m is defined by

$$m = v/c_r, \tag{3.2}$$

where c_r is the Rayleigh wave speed. This result, and others presented in this section, are all taken from the review article by Freund (1976).

Since they will be used in the sequel, we will specify the nondimensional universal functions Σ_{ij}. To do so, let

$$c_s = (\mu/\rho)^{1/2} \quad \text{and} \quad c_l = (2\mu(1-\nu)/[(1-2\nu)\rho])^{1/2} \tag{3.3}$$

be the velocities of shear and longitudinal waves, where ρ is the mass density. Let

$$\alpha_s = [1-(v/c_s)^2]^{1/2} \quad \text{and} \quad \alpha_l = [1-(v/c_l)^2]^{1/2} \tag{3.4}$$

and define θ_s and θ_l in terms of θ by

$$\tan\theta_s = \alpha_s \tan\theta \quad \text{and} \quad \tan\theta_l = \alpha_l \tan\theta. \tag{3.5}$$

Further, define w_s and w_l as functions of θ by

$$w_s = [1-(v\sin\theta/c_s)^2]^{1/4} \quad \text{and} \quad w_l = [1-(v\sin\theta/c_l)^2]^{1/4}. \tag{3.6}$$

Then,

$$\Sigma_{11} = \frac{1}{H}\left[(1+\alpha_s^2)(1+2\alpha_l^2-\alpha_s^2)\frac{\cos(\theta_l/2)}{w_l} - 4\alpha_l\alpha_s\frac{\cos(\theta_s/2)}{w_s}\right],$$

$$\Sigma_{12} = \frac{2\alpha_l(1+\alpha_s^2)}{H}\left[\frac{\sin(\theta_l/2)}{w_l} - \frac{\sin(\theta_s/2)}{w_s}\right], \tag{3.7}$$

$$\Sigma_{22} = \frac{1}{H}\left[-(1+\alpha_s^2)^2\frac{\cos(\theta_l/2)}{w_l} + 4\alpha_s\alpha_l\frac{\cos(\theta_s/2)}{w_s}\right]$$

and

$$\Sigma_{33} = \nu(\Sigma_{11}+\Sigma_{22}),$$

where

$$H = 4\alpha_s\alpha_l-(1+\alpha_s^2)^2. \tag{3.8}$$

Ahead of the tip, on $\theta = 0$, Σ_{22} is normalized to be unity for all m. In the limit $m \to 0$, the above reduce to the well-known expressions for a stationary crack. The function H vanishes for $v = c_r$ (i.e. $m = 1$), where the Rayleigh speed is approximately related to the shear wave speed by

$$c_r = \frac{0.862+1.14\nu}{1+\nu}c_s. \tag{3.9}$$

The elastic energy release-rate G, defined as the energy disappearing at the crack tip per unit of crack advance per unit length of front, is related to K by

$$G = f(m)\frac{(1-\nu^2)}{E}K^2, \tag{3.10}$$

where

$$f(m) = \frac{\alpha_l(v/c_s)^2}{(1-\nu)H}. \tag{3.11}$$

This function is plotted in Fig. 3 for $\nu = 0.3$.

In the elastic problem G and K are measures of the asymptotic near-tip field of the running crack. Solutions to elastic running crack problems provide the time dependence of K and G in terms of crack length history, applied stress history and overall geometry. In general these problems are extremely difficult, but some special problems have been solved. One example discussed by FREUND (1976) is the semi-infinite crack running into an infinite block of prestressed material. In this problem the dynamic stress intensity factor depends only on the current crack tip velocity according to the revealing form

$$K = k(m)K_S, \tag{3.12}$$

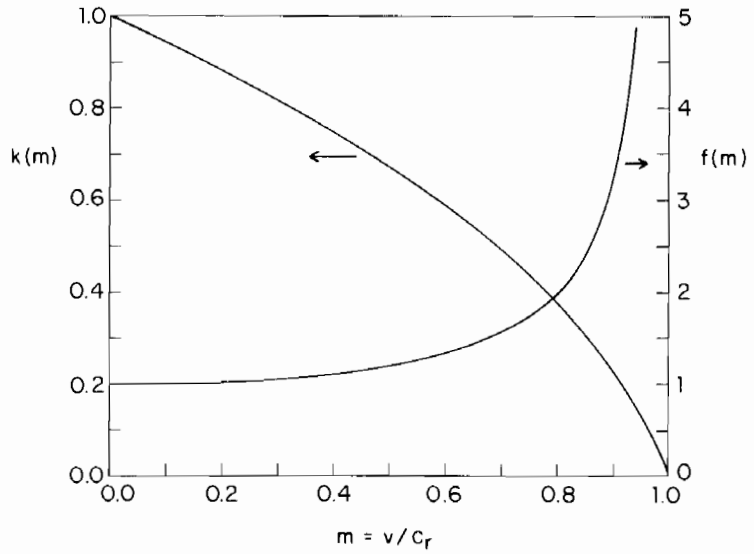

FIG. 3. $k(m)$ and $f(m)$ for $\nu = 0.3$.

where K_S is the *static stress intensity* factor calculated for a stationary crack in the prestressed material whose tip momentarily coincides with the running crack tip. The function $k(m)$ is plotted in Fig. 3 for $\nu = 0.3$. For future reference, we note that (3.12) is equivalent to

$$G = f(m)k^2(m)G_S, \tag{3.13}$$

where

$$G_S \equiv (1-\nu^2)K_S^2/E \tag{3.14}$$

is the associated *quasi-static energy release-rate*. The combination $f(m)k^2(m)$ is well approximated by $(1-m)$.

In the small scale yielding problem posed in the next section, G will be taken to prescribe the remote fields. However, it should always be borne in mind that G is related to the overall geometry, crack velocity and loading history through solution of the dynamic elastic problem, i.e. through results such as (3.13). We will have use for this relation in our discussion of crack propagation conditions.

4. Dynamic Steady-state Crack Growth in Small Scale Yielding

The crack tip is imagined to be running at a uniform velocity v and is assumed to have advanced a distance which is large compared to the size of the active plastic zone, the zone within which the plastic strain-rates do not vanish. Furthermore, the active plastic zone is assumed to be small compared to the zone of dominance of the dynamic singularity stress field (3.1), and the dynamic stress intensity factor K is assumed to be

maintained at a constant level. Under these conditions a steady-state, small scale yielding problem can be posed as depicted in Fig. 4. The active plastic zone travels along with the crack tip leaving behind a wake of residual plastic strains. Outside the wake, the remote stress field in this asymptotic small scale yielding problem is the dynamic singularity field specified by K, or, equivalently, by G via (3.10).

The analysis will be carried out within the context of small strain theory. The total strains, ε_{ij}, are related to the displacement, u_i, by

$$\varepsilon_{ij} = \tfrac{1}{2}(u_{i,j} + u_{j,i}) \tag{4.1}$$

and the momentum equations are

$$\sigma_{ij,j} = \rho \ddot{u}_i, \tag{4.2}$$

where the dot denotes the time-rate of change and Cartesian components are employed throughout the paper. The incremental form of these equations is the same with an extra time derivative of each term. The constitutive relation is specified by (2.5) and (2.6). In the steady-state problem, the time derivative of the Cartesian component of any vector or tensor associated with a material point is related to the x_1-gradient by

$$\dot{(\,)} \equiv \frac{\partial}{\partial t} = -v\frac{\partial}{\partial x_1}. \tag{4.3}$$

The following observation is essential to the subsequent analysis and discussion. As

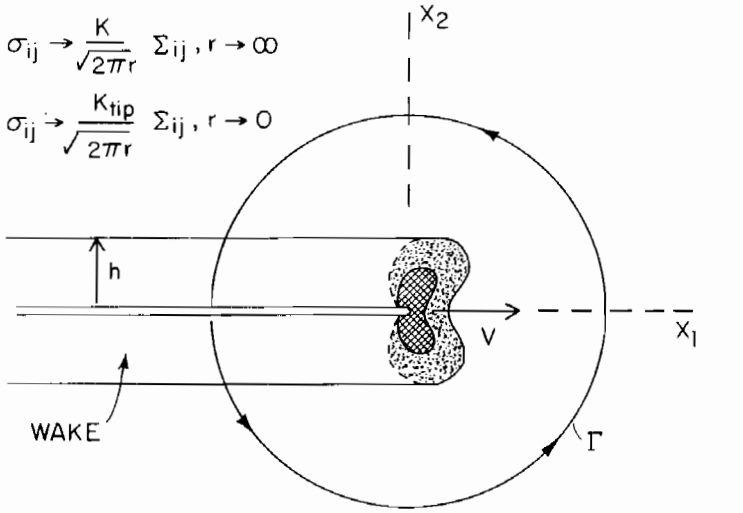

INTERMEDIATE TO LOW STRAIN-RATE ZONE ($\tau_y < \tau < \tau_t$)

HIGH STRAIN-RATE ZONE ($\tau > \tau_t$)

FIG. 4. Dynamic steady-state, small scale yielding crack propagation.

the crack tip is approached ($r \to 0$), the elastic strain-rates become unbounded in proportion to $\dot{\tau}$, while, by (2.5), the plastic strain-rates increase in direct proportion to τ. It follows from (4.3) that, if the stresses are unbounded at the tip, the elastic strain-rates are more singular than the plastic-rates and, therefore, that they dominate asymptotically as $r \to 0$. Consequently, the singularity field governing near-tip behaviour is the dynamic elastic field with precisely the same form as (3.1) except that the amplitude factor will be different. This observation holds for growth in elastic/power-law viscous materials as long as the stress exponent is less than 3, as shown by LO (1983). BRICKSTAD (1983) made use of the same singularity in his interpretation of crack propagation experiments. With K_{tip} as the dynamic stress intensity factor of the near-tip field,

$$\sigma_{ij} = \frac{K_{\text{tip}}}{\sqrt{(2\pi r)}} \Sigma_{ij}(\theta, m) \quad \text{as} \quad r \to 0. \tag{4.4}$$

The energy release-rate at the tip is denoted by G_{tip} and is given in terms of K_{tip} by the relation (3.10), i.e.

$$G_{\text{tip}} = f(m) \frac{(1-\nu^2)}{E} K_{\text{tip}}^2. \tag{4.5}$$

The solution to the steady-state problem will provide the relation between G_{tip} and G. An exact work-rate balance equation exists for the dynamic steady-state problem which relates G_{tip} to G. To derive this equation we now introduce a path-independent line integral for steady-state problems.

Given arbitrary material properties, rate-dependent or rate-independent, let U be the stress work density defined by

$$U = \int_0^{\varepsilon} \sigma_{ij} \, \mathrm{d}\varepsilon_{ij} \tag{4.6}$$

which, in general, depends on the history of deformation experienced by a given material point. Let T be the kinetic energy density, $T = \frac{1}{2}\rho \dot{u}_i \dot{u}_i$, and let Γ be any closed contour with outward pointing unit normal, n_i. The line integral

$$I = \int_{\Gamma} [(U+T)n_1 - \sigma_{ij} n_j u_{i,1}] \, \mathrm{d}s \tag{4.7}$$

is zero for all closed contours encircling no singularities. Path-independence is proved in the Appendix. This integral generalizes similar ones by SIH (1970) for linear elastic solids and by FREUND (1984) for nonlinear elastic solids. It is a special case of a path-independent integral for steady-state growth derived under somewhat more general conditions than those considered here by WILLIS (1975). We emphasize that the integral is limited to problems involving steady-state growth in the x_1-direction for which (4.3) holds. Otherwise, it is unrestricted in its application to solids with arbitrary properties, as long as these properties are independent of the x_1 coordinate.

For the present problem, where the material is characterized by the elastic/visco-plastic relation (2.5) and (2.6), we show in the Appendix that $I = G_{\text{tip}}$ when evaluated on a near-tip contour encircling the tip in a counterclockwise sense, such as that shown in

Fig. 4 but shrunk down to the tip. Evaluation on a remote contour encircling the tip in the same sense (again, see Fig. 4) gives

$$I = G - \int_{-h}^{h} U^* \, dx_2, \tag{4.8}$$

where

$$U^*(x_2) = \lim_{x_1 \to -\infty} U(x_1, x_2)$$

is the stress work density in the wake far behind the tip. From path-independence it follows that

$$G_{tip} = G - \int_{-h}^{h} U^* \, dx_2. \tag{4.9}$$

This work-rate balance is obvious from first principles in that the difference between the overall work and the work deposited in the wake in a unit advance of the crack under steady-state conditions is necessarily the work released at the tip. We also show in the Appendix that (4.9) can be rewritten as

$$G_{tip} = G - \frac{1}{v} \int_A \sigma_{ij} \dot{\varepsilon}^p_{ij} \, dA - \int_{-h}^{h} U_e^* \, dx_2, \tag{4.10}$$

where the area integral extends over the active plastic zone and where U_e^* is the residual elastic strain energy density in the remote wake.

5. Approximate Analysis of Steady-state High Velocity Crack Growth

A complete analysis of the steady-state small scale yielding problem posed in the previous section will require an extensive numerical analysis. Such an analysis will not be given in this paper. Instead, in this section we will carry out an approximate analysis which captures some of the qualitative features of the effect of plasticity on high speed crack growth. In particular, it will be shown that the present analysis is asymptotically rigorous under limiting conditions when the plastic dissipation is a sufficiently small fraction of the total energy release-rate.

The first step in the analysis is the determination of G_{tip} in terms of G using (4.10). To estimate the plastic dissipation in (4.10), *the plastic strain-rates will be computed using the near-tip stress distribution* (4.4). The amplitude of the near-tip stress fields, K_{tip}, is as of yet unknown and is related to G_{tip} by (4.5). Proceeding to calculate the plastic dissipation, one notes from (2.3) and (2.5) that

$$\sigma_{ij} \dot{\varepsilon}^p_{ij} = \tau F(\tau), \tag{5.1}$$

where τ is the effective shear stress defined in (2.3). Using the near-tip field (4.4) to calculate τ, one finds

$$\tau = \frac{K_{tip}}{\sqrt{(2\pi r)}} B(\theta, m), \tag{5.2}$$

where

$$B = \{\tfrac{1}{2}\Sigma_{11}^2 + \Sigma_{12}^2 + \tfrac{1}{2}\Sigma_{22}^2 + \tfrac{1}{2}[\nu^2 - \tfrac{1}{3}(1+\nu)^2](\Sigma_{11}+\Sigma_{22})^2\}^{1/2}. \tag{5.3}$$

Denote by $R(\theta)$ the radial distance to the boundary of the active plastic zone from the tip. Setting $\tau = \tau_y$ in (5.2) and solving for r gives

$$R = \frac{1}{2\pi}\left(\frac{K_{\text{tip}}}{\tau_y}\right)^2 B^2(\theta, m). \tag{5.4}$$

Then, by (5.1), the plastic dissipation term in (4.10) can be written as

$$\frac{1}{v}\int_A \sigma_{ij}\dot{\varepsilon}_{ij}^p \, dA = \frac{1}{v}\int_{-\pi}^{\pi} d\theta \int_0^{R(\theta)} \tau F(\tau) r \, dr. \tag{5.5}$$

Next, using (5.2) to change the integration with respect to r to an integration with respect to τ, one finds

$$\frac{1}{v}\int_A \sigma_{ij}\dot{\varepsilon}_{ij}^p \, dA = \frac{1}{2\pi^2 v} K_{\text{tip}}^4 \mathscr{B}(m) \int_{\tau_y}^{\infty} \tau^{-4} F(\tau) \, d\tau, \tag{5.6}$$

where

$$\mathscr{B}(m) = \int_{-\pi}^{\pi} B^4(\theta, m) \, d\theta. \tag{5.7}$$

Values of $\mathscr{B}(m)$ are included in Table 1 for $\nu = 0.29$.

The integral with respect to τ in (5.6) is independent of crack velocity. It is convenient to separate this integral into the contribution for $\tau \geqslant \tau_t$, corresponding to the highest strain-rate regime, and the remaining contribution according to

$$\int_{\tau_y}^{\infty} \tau^{-4} F(\tau) \, d\tau = \int_{\tau_t}^{\infty} \tau^{-4} F(\tau) \, d\tau + \int_{\tau_y}^{\tau_t} \tau^{-4} F(\tau) \, d\tau. \tag{5.8}$$

With F identified as (2.1), the first integral is readily integrated to give

$$\int_{\tau_t}^{\infty} \tau^{-4} F(\tau) \, d\tau = \frac{1}{3}\frac{\dot{\gamma}_t}{\tau_t^3} + \frac{1}{6}\frac{\dot{\gamma}_0}{\mu\tau_t^2}. \tag{5.9}$$

The contribution (5.9) from the regime in which plasticity is limited by phonon drag is large compared to the second contribution in (5.8). This is illustrated in Fig. 5 where the

TABLE 1. ($\nu = 0.29$)

m	0	0.1	0.2	0.3	0.4	0.5	0.6	0.7	0.8	0.9
$\mathscr{B}(m)$	0.202	0.205	0.217	0.241	0.285	0.367	0.548	1.06	3.42	38.7
$D(m)$	∞	0.441	0.224	0.155	0.124	0.110	0.111	0.135	0.233	0.892

$D(m) = 0.0438/m$ as $m \to 0$

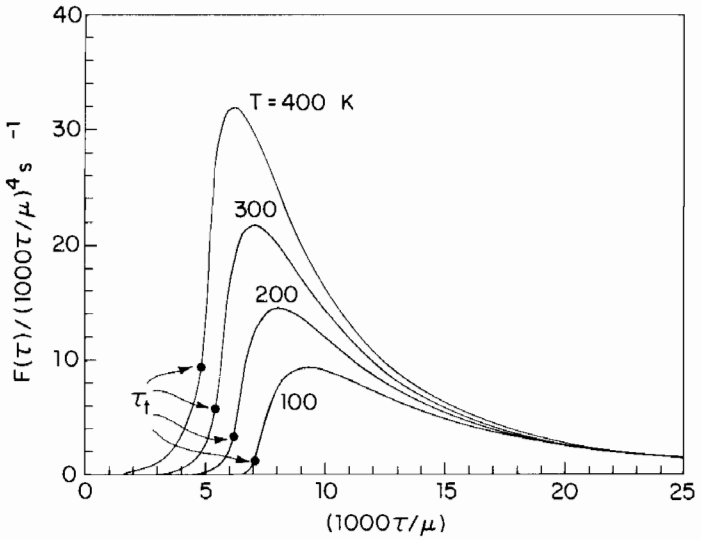

FIG. 5. Integrand of (5.8) based on the stress-strain-rate curves of Fig. 2. The high strain-rate regime corresponds to $\tau > \tau_t$.

integrand $\tau^{-4}F(\tau)$ is plotted as a function of τ (in an appropriately normalized fashion) using the curves of $\dot{\gamma}^p$ vs τ taken from the earlier example in Fig. 2. At each temperature, the solid dot denotes the transition between the intermediate strain-rate regime and the high strain-rate regime where $\tau = \tau_t$. The contribution of the second integral in (5.8) never exceeds 10% of (5.9), and to simplify the discussion it will be neglected entirely.

For simplicity, we will also neglect the term representing the residual elastic energy stored in the remote wake in (4.10). This term is generally fairly small and is asymptotically negligible for small plastic dissipation, as will be discussed further in the next section. Then, using (4.5) to express K_{tip} in terms of G_{tip} in (5.6), one can write (4.10) as

$$G_{\text{tip}} = G - D(m)\left(\frac{1}{3}\frac{\dot{\gamma}_0\sqrt{\mu\rho}}{\tau_t^2}\right)\left[1 + \frac{2\dot{\gamma}_t\mu}{\dot{\gamma}_0\tau_t}\right]G_{\text{tip}}^2, \tag{5.10}$$

where

$$D(m) = \frac{1}{\pi^2}\frac{\mathscr{B}(m)(c_s/c_r)}{m[(1-\nu)f(m)]^2}. \tag{5.11}$$

Values of the dimensionless function $D(m)$ are given in Table 1 and plotted in Fig. 6 for $\nu = 0.29$. Note that the minimum of D is $D_{\min} = 0.109$ occurring at $m = 0.55$. As $m \to 0$, $D = 0.0438/m$ for $\nu = 0.29$, and this formula is moderately accurate for m as large as 0.3.

Suppose the criterion for the crack to run under steady-state conditions is taken to be

$$G_{\text{tip}} = G_{\text{tip}}^c. \tag{5.12}$$

The critical energy release-rate, G_{tip}^c, represents the energy per unit of crack extension

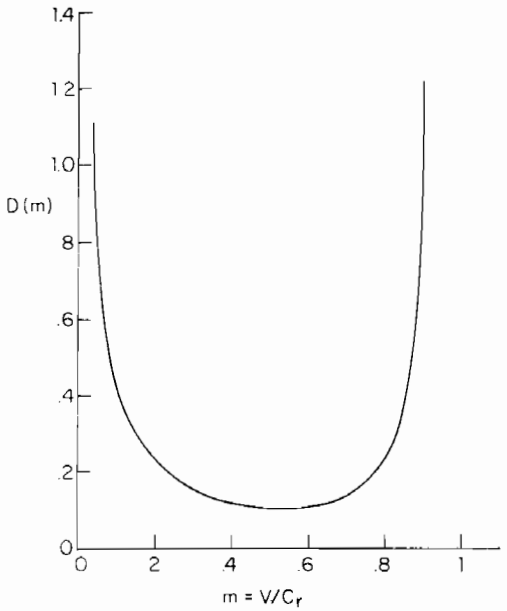

FIG. 6. $D(m)$ for $\nu = 0.29$. The minimum of D is 0.109 at $m = 0.55$.

absorbed by the fracture processes and not otherwise accounted for by the continuum analysis. In principle G^c_{tip} could be a function of v, but for simplicity of discussion it will be regarded here as a material constant independent of v. With (5.12) imposed, (5.10) gives the value of G required to propagate the crack at a given speed m, i.e.

$$\frac{G}{G^c_{\text{tip}}} = 1 + D(m)P_c, \tag{5.13}$$

where P_c is the nondimensional collection of material constants

$$P_c = \frac{1}{3}\frac{\dot{\gamma}_0\sqrt{(\mu\rho)}G^c_{\text{tip}}}{\tau_t^2}\left[1 + \frac{2\dot{\gamma}_t\mu}{\dot{\gamma}_0\tau_t}\right]. \tag{5.14}$$

Curves of G/G^c_{tip} as a function of m for various values of P_c are shown in Fig. 7. At a given value of P_c, the minimum value of G needed to drive the crack occurs for $m = 0.55$ with

$$\frac{G_{\min}}{G^c_{\text{tip}}} = 1 + 0.109P_c. \tag{5.15}$$

Combinations of G/G^c_{tip} and m falling below the appropriate curve in Fig. 7 correspond to $G_{\text{tip}} < G^c_{\text{tip}}$, while combinations above the curve give $G_{\text{tip}} > G^c_{\text{tip}}$. Assuming that the steady-state solutions have approximate validity under nonsteady conditions, this suggests that a running crack nucleated under combinations of G and m lying below the curves will decelerate until either a solution state on the contour is attained or the crack

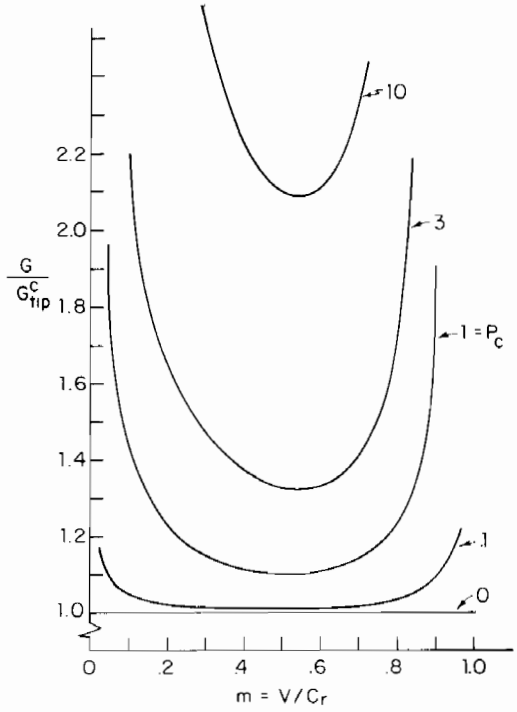

FIG. 7. G/G^c_{tip} as a function of m for various P_c ($\nu = 0.29$).

arrests, the latter possibility occurring if $m < 0.55$ at nucleation. Conversely, if nucleated with a combination lying above the curve, the crack will accelerate until a solution state on the right half of the solution curve is reached.

The above discussion becomes more relevant from a physical standpoint when an overall applied stress is regarded as being prescribed rather than the overall dynamic energy release-rate. For this purpose, imagine that a result such as (3.13) holds so that G_S, which is directly tied to the prescribed load, is regarded as being prescribed. The factor $f(m)k^2(m)$ in (3.13) is well approximated by $(1-m)$, and therefore we will use

$$G = (1-m)G_S. \tag{5.16}$$

Substituting (5.16) into (5.13), one obtains

$$\frac{G_S}{G^c_{\text{tip}}} = \frac{1}{1-m}\,[1 + D(m)P_c]. \tag{5.17}$$

Curves of G_S/G^c_{tip} as a function of m are shown in Fig. 8.

The minimum value of G_S, G^*_S, needed to drive the crack and the associated value of the normalized speed, m^*, are strong functions of P_c as can be seen in Fig. 9. For sufficiently small P_c (with $\nu = 0.29$),

$$G^*_S/G^c_{\text{tip}} \cong 1 + 0.419\sqrt{P_c} \quad \text{and} \quad m^* \cong 0.209\sqrt{P_c} \tag{5.18}$$

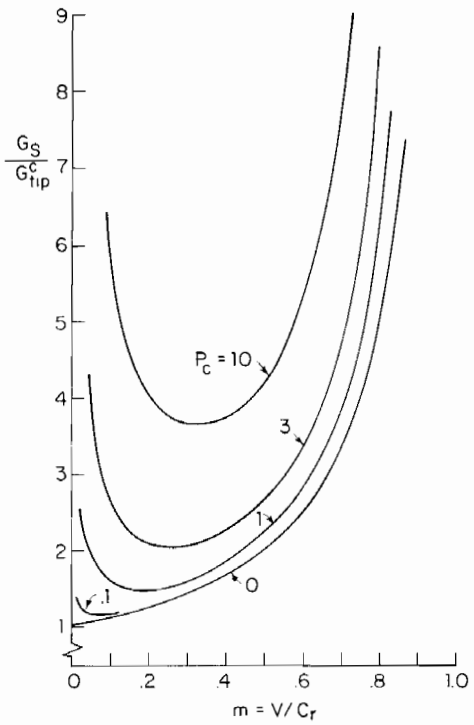

FIG. 8. G_S/G^c_{tip} as a function of m for various P_c ($\nu = 0.29$).

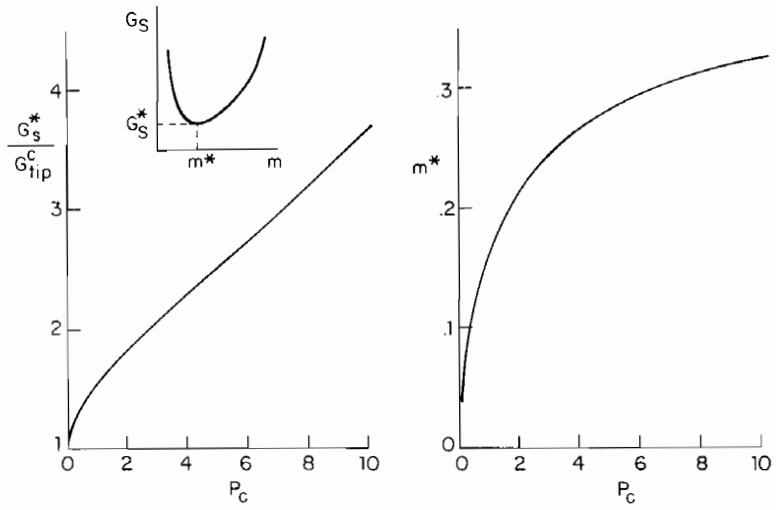

FIG. 9. Minimum value of G_S needed to drive the crack dynamically and associated value of m as functions of P_c ($\nu = 0.29$).

while for large P_c

$$G_S^*/G_{\text{tip}}^c \cong 1.67 + 0.187 P_c \quad \text{and} \quad m^* \to 0.40. \tag{5.19}$$

Implications of the strong dependence of G_S^* and m^* on the material parameter P_c will be discussed in Section 7.

6. Further Discussion of the Steady-state Problem

To gain further insight into the approximate solution it is useful to present the relation between G_{tip} and G in a slightly different manner. Following division by $G \neq 0$, the relation (5.10) has the form

$$G_{\text{tip}}/G = 1 - D(m) P (G_{\text{tip}}/G)^2, \tag{6.1}$$

where P is defined in terms of G (and *not* G_{tip}^c) as

$$P = \frac{1}{3} \frac{\dot\gamma_0 \sqrt{(\mu\rho)} G}{\tau_t^2} \left[1 + \frac{2\dot\gamma_t \mu}{\dot\gamma_0 \tau_t} \right]. \tag{6.2}$$

Solving (6.1) for G_{tip}/G, one finds

$$\frac{G_{\text{tip}}}{G} = \frac{(1+4DP)^{1/2} - 1}{2DP}. \tag{6.3}$$

Curves of G_{tip}/G as functions of P are shown in Fig. 10 for several values of m.

We now argue the following two points:

(1) The nondimensional variable

$$\alpha = \frac{\dot\gamma_t \mu^2 G}{v \tau_y^3} \tag{6.4}$$

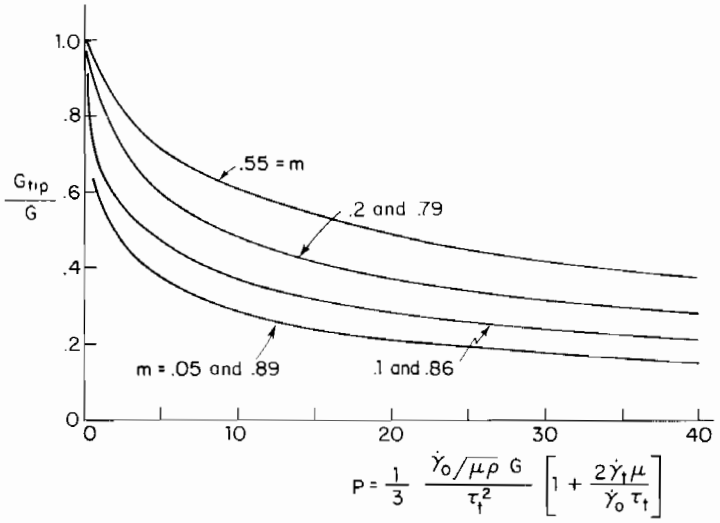

FIG. 10. G_{tip}/G as a function of P for various values of m.

provides a measure of whether or not the growth should be characterized as high strain-rate growth. For sufficiently small α the plastic strain accumulation essentially all occurs in the high strain-rate regime. The larger is α, the larger the contributions from the low and intermediate strain-rate regimes. When α is sufficiently large, low and intermediate strain-rate processes will dominate over most of the plastic zone. The zone of dominance of the singular field (4.4) is expected to shrink as α increases. For sufficiently large α we thus expect G_{tip} to lose its significance as the controlling near-tip parameter, and the growth should no longer be considered as high strain-rate growth.

(2) A second nondimensional variable,

$$\beta = \frac{\dot{\gamma}_0 \mu G}{v\tau_t^2}, \tag{6.5}$$

provides a measure of the range of validity of our approximate solution (6.3) or (5.10). For sufficiently small β, or equivalently for sufficiently small P/m, we will argue that our solution is asymptotically exact. This means that the initial slope of the relation between G_{tip}/G and P given by (6.3) and plotted in Fig. 10 is essentially exact.

6.1. *Characterization of high strain-rate growth*

Equation (1.2) provides an estimate of the plastic strain-rate $\dot{\gamma}^p$ in the outer region of the plastic zone, and thus α in (6.4) is proportional to the ratio of the transition strain-rate $\dot{\gamma}_t$ to $\dot{\gamma}^p$. If α is large enough, most of the plastic zone, except very near the tip, will be associated with low strain-rate deformation. Then it is to be expected that the crack growth will not be radically different from growth under rate-independent conditions. Growth of a sharp line-crack in a rate-independent plastic material is characterized by an inherently weaker singularity than the inverse square root singularity and the energy release-rate is identically zero according to such models. For such models alternative critical near-tip growth criteria must be assumed, such as a critical strain at some fixed distance ahead of the tip or an invariant opening profile near the tip (RICE, DRUGAN and SHAM, 1980). But if α is sufficiently small, the major portion of the plastic strain accumulation will take place in the high strain-rate regime, and the characterization of the near-tip field by G_{tip} is meaningful. This latter situation is what is meant by *high strain-rate crack growth* for present purposes. It may be, under certain circumstances, that high strain-rate growth conditions are met at velocities which are sufficiently low (e.g. $m < 0.2$) such that inertia effects are relatively unimportant. It remains for future work to determine the numerical value of α marking the transition to high strain-rate growth.

6.2. *Asymptotic validity of the present solution*

From (6.1) it can be seen that $G_{tip} \to G$ as $D(m)P \to 0$. Thus for sufficiently small $D(m)P$, the plastic dissipation term in (6.1) or (5.10) is well approximated by replacing G_{tip} by G. This is precisely equivalent to determining the plastic dissipation using the elastic field for the stresses (3.1) to calculate the plastic strain-rates rather than the near-tip stresses (4.4). In other words, the initial slope of the relation between G_{tip}/G and P is independent of whether the elastic stress field or the near-tip stress field is used to

calculate the plastic strain-rates, since the near-tip stress field asymptotes to the elastic field as $D(m)P \to 0$.

That this is to be expected can be seen in another way by making a consistency check showing that the elastic strain-rates dominate the plastic strain-rates when $D(m)P$ is sufficiently small, or equivalently when the parameter β in (6.5) is small. For order of magnitude purposes, we note that a typical elastic strain-rate quantity is given by

$$\dot{\gamma}^e = \frac{\dot{\tau}}{\mu} = -\frac{v}{\mu}\frac{\partial \tau}{\partial x_1} \propto \frac{v}{\mu}\frac{K}{r^{3/2}}, \tag{6.6}$$

assuming the elastic field to be predominant.

The distance from the tip to the boundary of the high strain-rate zone where $\tau = \tau_t$ is

$$R_t \propto (K/\tau_t)^2 \propto \mu G/\tau_t^2, \tag{6.7}$$

assuming m is not greater than about 0.4 or 0.5. Thus at the transition boundary where $\dot{\gamma}^p = \dot{\gamma}_t$,

$$\frac{\dot{\gamma}^p}{\dot{\gamma}^e} \propto \frac{\dot{\gamma}_t \mu^2 G}{v\tau_t^3} \equiv \beta\left(\frac{\dot{\gamma}_t \mu}{\dot{\gamma}_0 \tau_t}\right). \tag{6.8}$$

Well within the transition boundary for $\tau \gg \tau_t$,

$$\dot{\gamma}^p \cong \dot{\gamma}_0 \tau/\mu \propto \dot{\gamma}_0 K/(\mu r^{1/2}),$$

and thus

$$\frac{\dot{\gamma}^p}{\dot{\gamma}^e} \propto \frac{\dot{\gamma}_0 r}{v} \leqslant \frac{\dot{\gamma}_0 R_t}{v} \propto \frac{\dot{\gamma}_0 \mu G}{v\tau_t^2} \equiv \beta. \tag{6.9}$$

Experimental data for iron-based materials, such as that presented in Fig. 2, indicate that the nondimensional collection of material constants, $\dot{\gamma}_t \mu/(\dot{\gamma}_0 \tau_t)$, appearing in (6.8) is small compared to unity, typically on the order of 0.1 or less.† Thus if β is sufficiently small, the plastic strain-rates will be small compared to the elastic strain-rates everywhere within the high strain-rate portion of the plastic zone. Next note that

$$\frac{\alpha}{\beta} = \left(\frac{\dot{\gamma}_t \mu}{\dot{\gamma}_0 \tau_t}\right)\left(\frac{\tau_t}{\tau_y}\right)^3. \tag{6.10}$$

Since τ_t/τ_y is typically on the order of 2, the right hand side of (6.10) is on the order of unity or smaller. Thus, we can simultaneously ensure that α is small by requiring β to be small. Moreover, it is easy to show that sufficiently small α ensures that the plastic strain-rates in the outer portion of the plastic zone are small compared to the elastic strain-rates. In conclusion, then, the elastic strain-rates will dominate the plastic strain-rates everywhere when β is sufficiently small. To finish the argument we note that

$$\beta \propto P/m, \tag{6.11}$$

assuming the collection of terms $\dot{\gamma}_t \mu/(\dot{\gamma}_0 \tau_t)$ can be neglected in the definition of P in (6.2). For m less than about 0.2 or 0.3, $D \propto 1/m$ and thus β goes to zero in proportion to DP.

† Note from (2.1) that $\dot{\gamma}_0 \tau_t/\mu$ corresponds to the plastic strain-rate increase due to a doubling of stress above τ_t. This increase is typically at least an order of magnitude larger than $\dot{\gamma}_t$.

For sufficiently small β the plastic strain-rate is dominated by the elastic strain-rate everywhere in the plastic zone, and our calculation of the plastic dissipation in the energy balance (4.10) is asymptotically correct. Finally, it can be shown that the term representing the residual elastic energy density in the wake is of order β relative to the plastic dissipation term. Consequently it makes no contribution to the initial slope of the relation of G_{tip}/G to P. This concludes our argument that the initial slope is given exactly by our analysis.

At arbitrary values of P, we expect the approximate relation (6.3) to overestimate G_{tip}/G since the near-tip stress field (4.4), on which the calculation is based, almost certainly underestimates the stresses in the outer portion of the plastic zone. In other words, our approximate analysis has underestimated the plastic dissipation, as well as having neglected the residual elastic energy in the wake. Further work of a numerical character will be needed to establish the range of the β-parameter over which the present relatively simple solution is a good approximation and to obtain accurate results outside that range.

7. Application of Theory to Macroscopic Cleavage Crack Growth in Mild Steel

As a representative example we consider dynamic growth of a macroscopic crack in mild steel which is assumed to have a transition stress, τ_t, which varies with temperature as shown in Fig. 11. For temperatures above 200 K, τ_t has been taken from the data for the fine grained mild steel given in Fig. 6 of the paper by Campbell and Ferguson (1970).

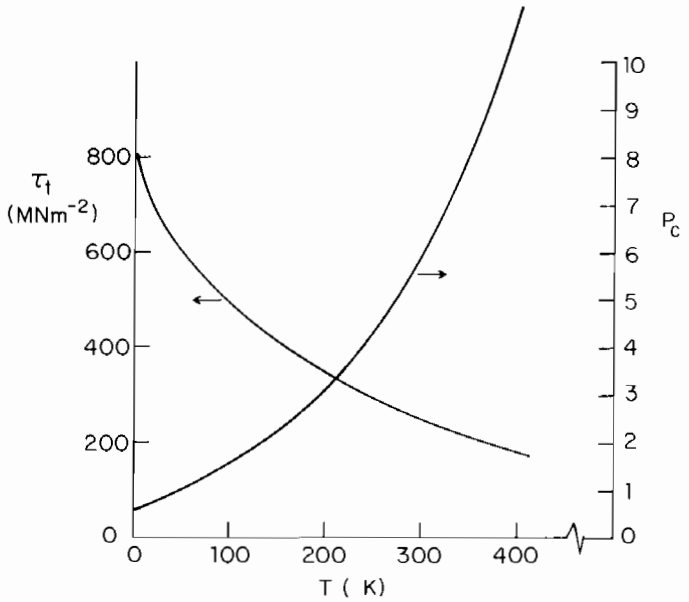

Fig. 11. Representative temperature dependence of τ_t and P_c for mild steel. See text for origin of data.

The limit as $T \to 0$ is taken as $\tau_t = 810$ MN m^2 which emerges from data given by FROST and ASHBY (1982) for steels. The variation of τ_t between 0 K and 200 K is taken as a smooth interpolation between these two sets of data. Between 0 K and room temperature, τ_t drops by about a factor of three which is typical of the drop in the low strain-rate yield stress, τ_y, for mild steel over this same temperature range.

A representative value of K_{Ic} for mild steel at 0 K is 22 MNm$^{-3/2}$ (20 ksi in$^{1/2}$). If this value is identified with the minimum value, K_S^*, needed to drive the crack dynamically, then from (3.14) the associated value of G_S^* at 0 K is 2.37×10^3 Nm^{-1}. Given G_S^*, together with the other material constants at 0 K that enter into the definition of P_c, one can use Fig. 9 to infer G_{tip}^c. With $\mu = 7.26 \times 10^4$ MN m^{-2}, $\rho = 7.2 \times 10^3$ Ns^2 m^{-4}, $\dot{\gamma}_0 = 3 \times 10^7$ s^{-1}, $\tau_t = 810$ MN m^{-2}, and neglecting $\dot{\gamma}_t \mu/(\dot{\gamma}_0 \tau_t)$, one obtains

$$G_{tip}^c = 1.73 \times 10^3 \text{ Nm}^{-1}. \tag{7.1}$$

In what follows, we will assume that G_{tip}^c is independent of T even though the near-tip cleavage processes in a polycrystalline metal are expected to have some temperature dependence. Specifically, the energy absorbed in ductile tearing of the uncleaved ligaments connecting cleavage facets on neighboring parallel planes appears to increase strongly with temperature in the vicinity of the ductile-brittle transition.

Given the temperature variation of τ_t in Fig. 11, the temperature variation of μ (which is relatively unimportant) given by Frost and Ashby, and the value of G_{tip}^c in (7.1), the temperature variation of P_c is that shown in Fig. 11. Figure 10 can now be used to crossplot the variations of G_S^* and m^* as functions of T, and the results are shown in Fig. 12. Over the range of temperature shown, G_S^* is seen to increase by a factor of 3 while m^* increases from about 0.125 to 0.33. The most important point, which is seen most clearly in Fig. 8, is the elimination of accessible propagation states as P_c increases.

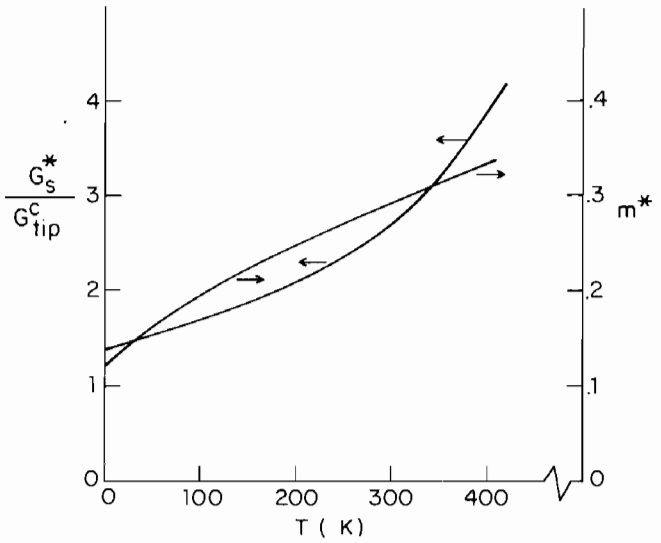

FIG. 12. Minimum G_S needed to drive macroscopic crack dynamically in mild steel and associated normalized crack speed as functions of temperature.

Assume again for the purpose of discussion that the steady-state solution has approximate validity under nonsteady conditions. Then, for example, if $P_c = 1$ a crack nucleated at $m = 0.1$ will run if $G_S/G^c_{\text{tip}} \geqslant 1.6$, while $G_S/G^c_{\text{tip}} \geqslant 6$ is required when a crack is nucleated with $m = 0.1$ if $P_c = 10$. By the same token, if $G_S/G^c_{\text{tip}} = 3$, for example, a crack will run at initiation velocities as low as $m = 0.02$ if $P_c = 1$; the crack cannot be made to run at all if $P_c = 10$.

In the above discussion any dependence of G^c_{tip} on temperature has been disregarded. The steep increase in fracture toughness observed experimentally as the ductile–brittle transition temperature is approached is most likely associated with an increase of G^c_{tip} with temperature in the vicinity of the transition, within the context of the present model. That is, increases in G^c_{tip} with temperature would give rise to a stronger temperature dependence of P_c than illustrated in Fig. 11 and a correspondingly stronger increase in G^*_S with temperature.

Acknowledgement

The work of LBF was supported by the Materials Research Laboratory at Brown University, by the National Science Foundation under Grant MEA-82-10931, and by Harvard University through a visiting appointment in the Division of Applied Sciences. The work of JWH was supported in part by the National Science Foundation under Grants DMR-80-20247 and MEA-82-13925, and by the Division of Applied Sciences, Harvard University.

References

Brickstad, B.	1983	*J. Mech. Phys. Solids* **31,** 307–327.
Budiansky, B., Hutchinson, J. W. and Lambropoulos, J. C.	1983	*Int. J. Solids Structures* **19,** 337–355.
Campbell, J. D. and Ferguson, W. G.	1970	*Phil. Mag.* **21,** 63–82.
Clifton, R. J.	1983	*J. Appl. Mech.* **50,** 941–952.
Freund, L. B.	1976	In *Mechanics Today, Vol. 3*, ed. S. Nemat-Nasser, pp. 55–91, Pergamon Press, Oxford.
Freund, L. B.	1984	In *Fundamentals of Deformation and Fracture*, ed. K. J. Miller, Cambridge University Press, to appear.
Frost, H. J. and Ashby, M. F.	1982	*Deformation-Mechanism Maps*, Pergamon Press, Oxford.
Lo, K. K.	1983	*J. Mech. Phys. Solids* **31,** 287–305.
Rice, J. R., Drugan, W. J. and Sham, T.-L.	1980	In *Fracture Mechanics: Twelfth Conference*, ASTM STP 700, American Society for Testing and Materials, 189–221.
Sih, G. C.	1970	In *Inelastic Behavior of Solids*, eds. M. F. Kanninen *et al.*, pp. 607–633, McGraw-Hill, New York.
Willis, J. R.	1975	In *Mechanics and Physics of Fracture*, pp. 57–67, The Metals Society.

APPENDIX

A path-independent integral for steady-state crack growth

The path-independent line integral given below is a consequence of momentum balance and the assumed steady-state character of the solution. No constitutive restrictions are necessary; the integral applies to rate-dependent or rate-independent nonlinear materials. With U as the stress work density defined in (4.6) and $T = \frac{1}{2}\rho\dot{u}_i\dot{u}_i$ as the kinetic energy density, we first demonstrate the path-independence of the line integral defined in (4.7) for all closed contours Γ which contain no singularities. Essential to the path-independence is that the steady-state relation between the time derivative and the x_1-gradient given by (4.3) hold. Steady-state solutions will only exist for special geometries and loadings. Our application of the integral is to solids with initially homogeneous properties, but steady-state solutions can exist in certain instances when initial material properties vary in the x_2-direction, as long as there is no x_1-variation. The present derivation is made within the context of small strain and small rotation theory, but it can be generalized to a full finite deformation formulation.

Let Γ surround the area A_Γ, which is assumed to contain no singularities. In the derivation which follows the divergence theorem, the steady-state relation (4.3), and momentum (4.2) are used in ways which will be obvious in their context:

$$\begin{aligned}\int_\Gamma (U+T)n_1\,\mathrm{d}s &= \int_{A_\Gamma} (U_{,1}+T_{,1})\,\mathrm{d}A = -v^{-1}\int_{A_\Gamma}(\dot{U}+\dot{T})\,\mathrm{d}A\\ &= -v^{-1}\int_{A_\Gamma}(\sigma_{ij}\dot{\varepsilon}_{ij}+\rho\dot{u}_i\ddot{u}_i)\,\mathrm{d}A\\ &= \int_{A_\Gamma}(\sigma_{ij}u_{i,j1}+\rho\ddot{u}_i u_{i,1})\,\mathrm{d}A\\ &= \int_{A_\Gamma}[(\sigma_{ij}u_{i,1})_{,j}-(\sigma_{ij,j}-\rho\ddot{u}_i)u_{i,1}]\,\mathrm{d}A\\ &= \int_\Gamma \sigma_{ij}n_j u_{i,1}\,\mathrm{d}s. \end{aligned} \tag{A.1}$$

This establishes path-independence. Application of the divergence theorem requires that the solution be free of discontinuities such as shocks. Shock-like discontinuities are common in wave propagation problems, including dynamic crack propagation problems. However, the equations governing the steady-state growth of a crack in a linear, isotropic elastic material are elliptic, and therefore discontinuity-free, as long as the crack velocity is less than the Rayleigh speed. The present application to crack growth in elastic/visco-plastic solids is also governed by elliptic equations.

In its quasi-static limit ($T = 0$), the integral was applied by BUDIANSKY, HUTCHINSON and LAMBROPOULOS (1983) to analyze steady-state crack growth in a special class of two-phase composite ceramic systems. The integral was used to connect near-tip and remote stress fields when a zone of martensitic-like transformation is induced in one of the phases by the high stresses near the tip. A derivation of the integral for steady-state dynamic growth was first given by SIH (1970) for linear elastic materials and later by FREUND (1984) for nonlinear elastic solids. Although nonlinear elasticity was invoked by Freund, a careful inspection reveals that his derivation goes through for arbitrary material behavior if the energy density function is interpreted as the stress work density. WILLIS (1975) gives a more general derivation than the present one which includes heat flux, and is also valid for arbitrary materials.

For the small scale yielding, steady-state problem, we define I as in (4.7) where Γ now encircles the crack tip in a counterclockwise sense. To relate I to the near-tip fields, deform Γ to the rectangular contour centered at the tip with sides parallel to the axes such that A_Γ is the region:

$-\delta_1 \leqslant x_1 \leqslant \delta_1$ and $-\delta_2 \leqslant x_2 \leqslant \delta_2$. Then shrink the contour down to the tip to get

$$\begin{aligned} I &= \lim_{\delta_1 \to 0} \lim_{\delta_2 \to 0} -2 \int_{-\delta_1}^{\delta_1} (\sigma_{12} u_{1,1} + \sigma_{22} u_{2,1}) \, dx_1 \\ &= \lim_{\delta_1 \to 0} \lim_{\delta_2 \to 0} 2v^{-1} \int_{-\delta_1}^{\delta_1} (\sigma_{12} \dot{u}_1 + \sigma_{22} \dot{u}_2) \, dx_1 \end{aligned} \tag{A.2}$$

where, by the symmetry of mode I, the integral can be evaluated on the side $x_2 = \delta_2$. For a near-tip field which asymptotes to (4.4), FREUND (1976, p. 70) has shown that the right hand side of (A.2) equals G_{tip} given by (4.5). As already discussed, the plastic strain-rates are dominated by the elastic strain-rates as $r \to 0$ and make no contribution to (A.2).

Next, deform Γ to a circular contour centered at the tip with radius r which is large compared to the active plastic zone. On this contour the contributions decouple into two parts as $r \to \infty$, one from the asymptotic elastic solution (3.1) outside the wake and one from the wake. The behavior in the remote wake is equivalent to that in a layer of thickness h with residual plastic strains, which are independent of x_1, attached to a semi-infinite half-space. The non-zero stress component within the layer is σ_{11}, and the strain component ε_{11} is the same as in the half-space, i.e. $\varepsilon_{11} \to 0$ as $r \to \infty$ in the wake. The stress distribution outside the layer is unaffected by the existence of the residual stress in the layer. The contribution to I on the remote circular contour from the region outside the wake is therefore just G as $r \to \infty$. The contribution from the wake itself in mode I is

$$\lim_{x_1 \to -\infty} -2 \int_0^h U(x_1, x_2) \, dx_2, \tag{A.3}$$

since T and $\sigma_{ij} n_j u_{i,1}$ vanish on Γ in the remote wake. The latter follows from the fact that $\mathbf{n} = (-1, 0)$ on Γ as $x_1 \to -\infty$ and, furthermore, that σ_{12} and $u_{1,1} = \varepsilon_{11}$ vanish in the remote wake. The two contributions to I combine to give (4.8), with (4.9) following from path-independence.

Lastly, we note that (4.10) can be obtained from (4.9) in several ways. Perhaps the simplest is as follows. Split U into the elastic energy density, U^e, and the plastic work density, U^p, according to

$$U^e = \int \sigma_{ij} \, d\varepsilon^e_{ij} \quad \text{and} \quad U^p = \int \sigma_{ij} \, d\varepsilon^p_{ij}. \tag{A.4}$$

Then note that the area integral in (4.10) can be written as

$$\begin{aligned} \int_A \sigma_{ij} \dot{\varepsilon}^p_{ij} \, dA = \int_A \dot{U}^p \, dA &= -v \int_A U^p_{,1} \, dx_1 \, dx_2 \\ &= \lim_{x_1 \to -\infty} v \int_{-h}^{h} U^p(x_1, x_2) \, dx_2, \end{aligned} \tag{A.5}$$

where the integration with respect to x_1 has been performed using the fact that $U^p = 0$ on the leading edge of the active plastic zone. It now follows immediately that (4.10) is equivalent to (4.9).